Universidad de Alcalá
BIBLIOTECA

Document downloaded from the institutional repository of the University of Alcala: http://dspace.uah.es/

This is the pre-peer reviewed version of the following article: Núñez-Cascajero, A., Jiménez-Rodríguez, M., Monroy, E., González-Herráez, M. and Naranjo, F. B. (2017), "Development of AlInN photoconductors deposited by sputtering", Physica Status Solidi A, 1600780. doi:10.1002/pssa.201600780, which has been published in final form. This article may be used for non-commercial purposes in accordance with Wiley Terms and Conditions for Self-Archiving.

Available at http://dx.doi.org/10.1002/pssa.201600780

© 2017 Wiley

(Article begins on next page)

This work is licensed under a

Creative Commons Attribution-NonCommercial-NoDerivatives 4.0 International License.

Review copy – not for distribution

Development of AlInN photoconductors deposited by sputtering

Arántzazu Núñez-Cascajero[*,1], Marco Jiménez-Rodríguez[1], Eva Monroy[2,3], Miguel González-Herráez[1], Fernando B. Naranjo[1]

[1] Grupo de Ingeniería Fotónica, Universidad de Alcalá, Departamento de Electrónica, Alcalá de Henares, Madrid, Spain
[2] Université Grenoble-Alpes, 38000 Grenoble, France
[3] CEA-Grenoble, INAC-PHELIQS, 17 av. des Martyrs, 38000 Grenoble, France

Received ZZZ, revised ZZZ, accepted ZZZ
Published online ZZZ (Dates will be provided by the publisher.)

Keywords: III-nitride, sputtering, characterization, device

In this work, we have developed photoconductor devices based on $Al_{0.39}In_{0.61}N$ layers grown on sapphire by reactive radio-frequency magnetron sputtering. The fabricated devices show a sublinear dependence of the photocurrent as a function of the incident optical power. The above-the-band-gap responsivity reaches 7 W/A for an irradiance of 10 W/m^2 (405 nm wavelength). The response decreases smoothly for below-the-bandgap excitation, dropping by more than an order of magnitude at 633 nm. The devices present persistent photoconductivity effects associated to carrier trapping at grain boundaries.

Copyright line will be provided by the publisher

1 Introduction AlInN is a direct band gap semiconductor whose band gap can be tuned with the indium composition from the near-infrared (0.7 eV for InN [1]) to the mid-ultraviolet (6.2 eV for AlN [2]). It presents high radiation hardness, and high thermal and chemical stability. These properties make it interesting for applications in light-emitting devices, solar cells and opto/chemical sensing [3-6]. This material can be synthesized by different methods, such as molecular beam epitaxy (MBE) [7,8], metalorganic chemical vapour deposition (MOCVD) [9,10] or radio-frequency (RF) reactive sputtering [11-13]. Unlike MBE or MOCVD, sputtering is a low cost technique which allows the deposition of III-nitrides at low temperature (even at room temperature), making it possible to use flexible substrates. Layers synthesized at low temperature do not present phase separation due to the immiscibility gap between constituents, since the growth is carried out far from thermal equilibrium. However, this technique presents disadvantages such as the polycrystalline nature of the layers and their high residual impurity concentration.

Photoconductors are the simplest semiconductor detectors; their operation is related to a light-induced change in the device conductivity [14]. There is extensive work on photoconductors based on (Al)GaN materials [14-20], but, as far as we know, there is no report on AlInN photoconductors.

In this work, we describe the performance of low-cost $Al_{0.39}In_{0.61}N$ photoconductors fabricated on RF-sputtered layers. They present an absorption spectral cut-off related to the semiconductor band gap (ultraviolet-to-red contrast > 10), high gain, and sublinear behaviour with the optical power.

2 Device fabrication and experimental setup Details on the optimization of AlInN deposition by RF reactive magnetron sputtering were previously reported elsewhere [11]. The AlInN layers used in this study were grown on c-sapphire under the previous optimized condi-

Copyright line will be provided by the publisher

tions: the substrate temperature was fixed at 450°C, measured with a K-type thermocouple placed in direct contact with the substrate holder. The power applied to the In and Al targets was 40 W and 150 W, respectively, and the layers were grown using pure nitrogen plasma. The substrates were chemically cleaned and degassed prior to growth. The deposition time was set to 42 to 150 minutes to achieve samples with thickness of 80 and 350 nm, respectively. The structural properties of the layers were studied by X-ray diffraction (XRD) measurements by a PANalytical X'Pert PRO MRD diffractometer. The sample morphology was studied by atomic force microscopy (AFM) in a Nanoscope IIIa system operated in the tapping mode. The optical properties were assessed by the analysis of transmittance measurements, using a 20 W halogen lamp as excitation source.

Once the layers were characterized, they were cut into 1x0.5 cm^2 bars, and they were processed into devices using indium contacts with an interdigitated pattern as ohmic contact. The contacts consisted of molten indium applied using a soldering iron. The distance between fingers and the finger thickness was of 1 mm in both cases. Current-voltage (I-V) characteristics confirmed that the contacts were ohmic. Resistances of 1.0 kΩ and 120 Ω were measured for devices fabricated on 80 and 350 nm thick layers, respectively. Figure 2 shows the I-V characteristics of the In contacts measured under dark conditions. Linear I-V characteristics were obtained in all cases, confirming the ohmic behavior of the contacts.

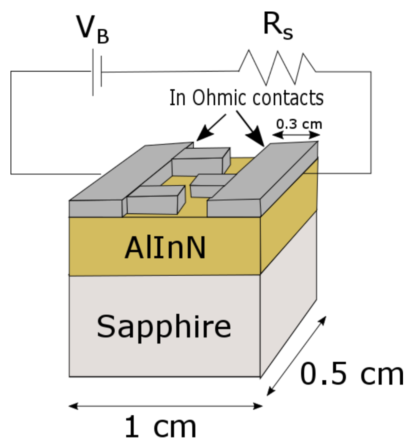

Figure 1 AlInN photoconductor structure.

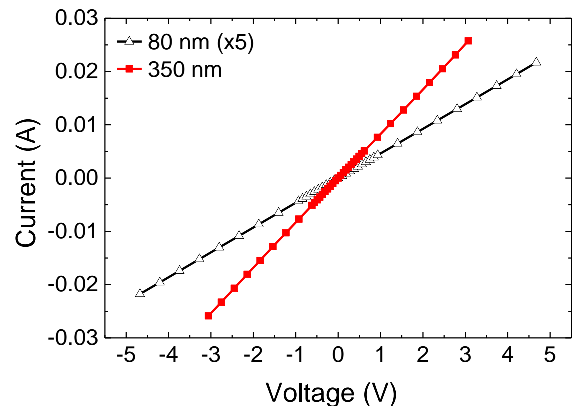

Figure 2 I-V characteristics of the samples under study showing the linear relationship between applied voltage and the measured current. The data of the 80 nm-thick sample appears multiplied by 5.

For the characterization of the photoconductors, they were connected to a 5 V bias source, in series with a load resistance which was chosen to be significantly smaller than the device resistance (see figure 1). The change in resistivity of the device under illumination was probed by measuring the variation of the voltage drop across the load resistance. The variation of responsivity as a function of the impinging optical power was measured by excitation with laser sources (GaN laser diode at 405 nm and HeNe laser at 633 nm) focused on the device. The spectral response was measured using a 20 W halogen lamp and an Oriel Instruments Cornerstone 130 1/8m monochromator. The photocurrent was recorded after keeping the samples in the dark for a long time (>12 h), and always from low optical power to high optical power and from long wavelengths to short wavelengths, to minimize persistent photoconductivity effects. The photocurrent measurement was corrected by the spectral response of the lamp taking the dependence of the responsivity on the optical power into account.

3 Results and discussion

3.1 Layer properties The AlInN layers were characterized to assess their structural, morphological and optical properties, prior to device fabrication. XRD measurements showed that all the layers present (0001)-oriented wurtzite structure. As an example, figure 3 presents the 2θ/ω scan of the 80 and 350 nm thick AlInN layers. Only the (0002) and (0004) diffraction peaks of AlInN and the (0006) line of the sapphire substrate are observed, which implies that phase separation is negligible. The shoulders that appear around the AlInN diffraction peaks are maybe related with In_2O_3 formed in the surface of the layer. The aluminium mole fraction calculated from the XRD measurements by using the Vegard's law and assuming fully relaxed layers is of 0.39.

Copyright line will be provided by the publisher

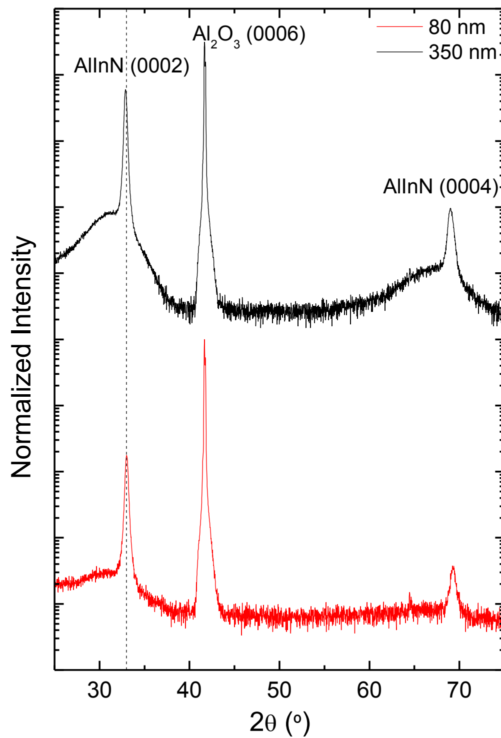

Figure 3 XRD 2θ/ω scan of the 80 and 350 nm thick AlInN samples deposited on c-sapphire.

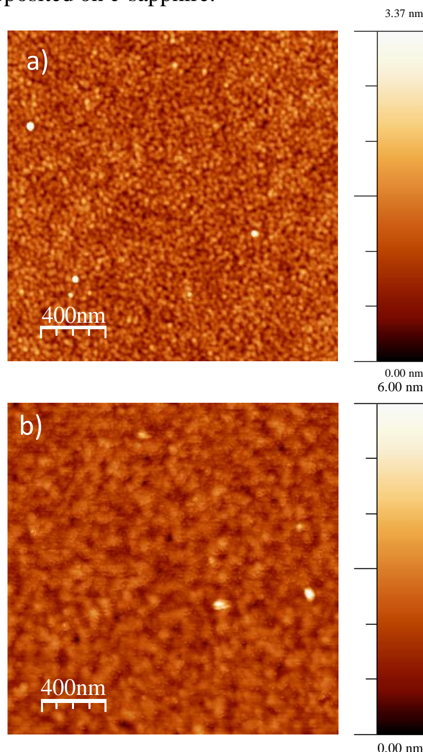

Figure 4 AFM images of the: a) 80 nm thick and b) 350 nm thick AlInN layers.

The surface morphology was studied by AFM. A root-mean-square (rms) surface roughness of 0.4 ± 0.1 nm was measured in 2x2 μm^2 images for both samples, with a slight increase of the grain size for the thicker layer (see figure 4).

Finally, the optical properties of the layers were analysed by optical transmittance measurements. Figure 5 shows the transmittance spectrum of the thickest layer (350 nm). The band gap energy has been estimated through a sigmoidal approximation [21], obtaining a value of ~ 2.15 eV (576 nm), which is consistent with a blue-shift of the expected bandgap due to a Burstein-Moss effect, as the expected carrier concentration in the layers is in the range of $1.6{\cdot}10^{20}$ cm^{-3} [11]. This band gap energy is in agreement with other results in AlInN layers grown by magnetron sputtering and presenting similar alloy composition [22]. An absorption band edge broadening of 0.3 eV has been estimated, broader than the 0.1 eV typically obtained for InN [11].

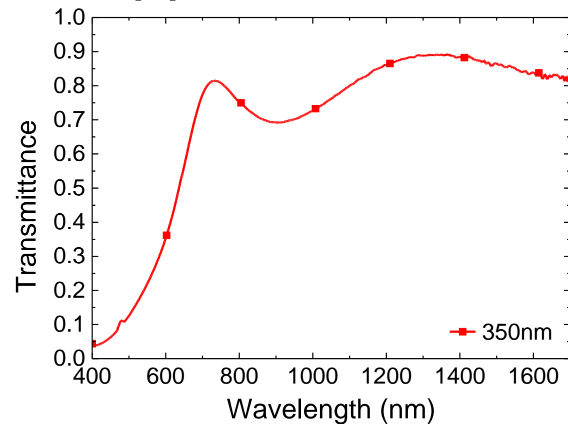

Figure 5 Room temperature transmittance spectra of the 350 nm thick sample.

3.2 Device characterization The responsivity as a function of the impinging optical power was measured with the results presented in figure 5. The dependence of the responsivity on the optical power can be described by $R \propto P_{opt}^{-\gamma}$ both for excitation at 405 nm (above the band gap) and at 633 nm (below the band gap). The γ parameter is in the range of 0.79 to 0.96, depending on the sample, in agreement with data in AlGaN-based photoconductors [17].

Copyright line will be provided by the publisher

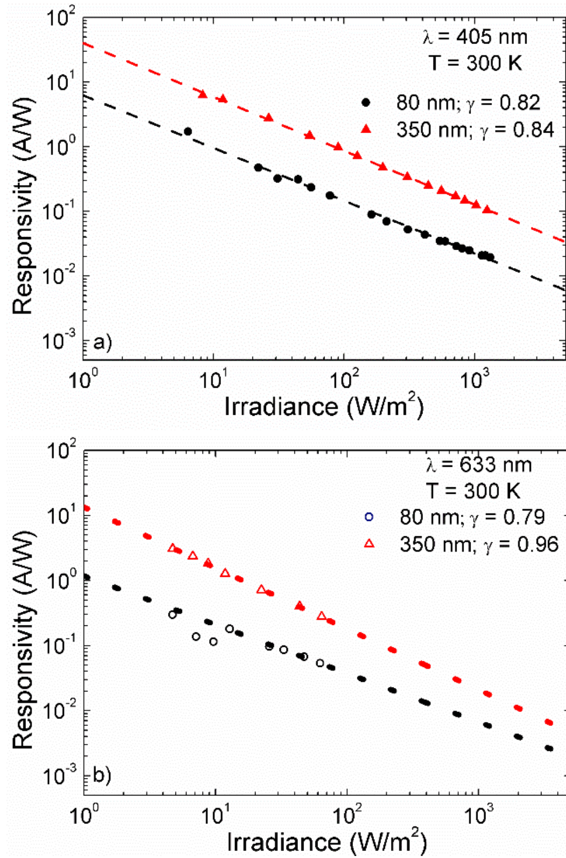

Figure 6 Responsivity as a function of the optical power for all the samples under study: a) using a 405 nm incident wavelength and b) using a 633 nm incident wavelength.

The devices present gain for low irradiance. For instance, at 10 W/m^2 and for an incident wavelength of 405 nm, the gain is 3.1 and 22 for the 80 and 350 nm thick layers, respectively.

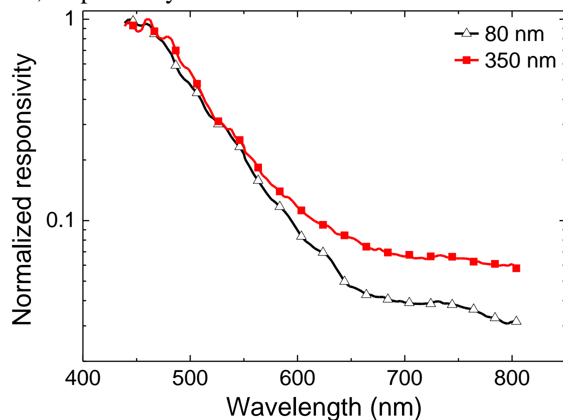

Figure 7 Spectral response of photoconductors fabricated on AlInN layers with different thicknesses.

Figure 7 shows the spectral response of the analysed devices. Below the band gap, the responsivity decays smoothly, which is explained by the presence of alloy inhomogeneities [19] and traps associated to the grain boundaries [23]. Nevertheless, the contrast between the responsivity at wavelengths above and below band gap can be larger than one order of magnitude, which compares favourably with AlGaN photoconductors [24]. Also it is observed that the absorption maximum is well above the band gap. This blue shift of the photoresponse might be related with the high carrier concentration, due to the Burstein-Moss effect [18].

Finally, we have studied the photoconductivity decay time, i.e. the evolution of the sample conductivity in the dark after being illuminated. Figure 8 shows the evolution of the photocurrent after switching off the illumination at time = 0. The decay is slow (hours) and strongly non-exponential. This phenomenon is known as persistent photoconductivity and it is generally associated to carrier trapping at the grain boundaries [17, 24].

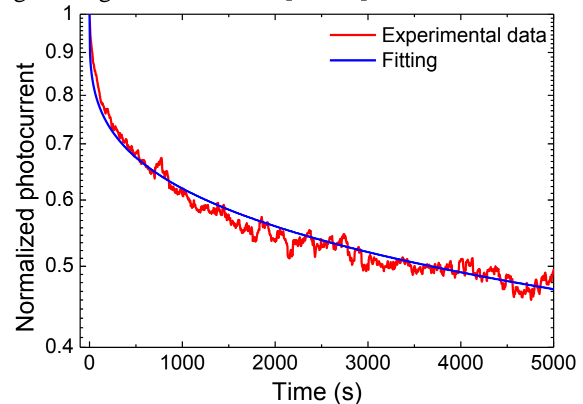

Figure 8 Photoresponse decay of the 350 nm-thick AlInN photoconductor at room temperature. The blue line is a fit of the experimental data to Eq. (1).

As shown in figure 8, the experimental values can be fitted to a stretched exponential function:

$$I_{ph}(t) = I_{ph0}e^{\left(\frac{-t}{\tau}\right)^{\beta}} \tag{1}$$

where I_{ph0} is the value of the photocurrent when the light is switched off, τ is the decay time constant and β is the decay exponent. The obtained values of the fitting parameters (τ = 13400 s and β = 0.28) are in agreement with the ones obtained for AlGaN photoconductors grown by MBE [18].

4 Conclusions We have demonstrated the fabrication of $Al_{0.39}In_{0.61}N$-on-sapphire photoconductors by reactive RF magnetron sputtering. The devices present high above-the-bandgap responsivity at low irradiance, reaching 7 W/A for an irradiance of 10 W/m^2. The response is strongly sublinear with the optical power, and it decreases smoothly for below-the-bandgap excitation, dropping by more than an order of magnitude at 633 nm. The devices present persistent photoconductivity effects. The general

Copyright line will be provided by the publisher

performance of these low-cost devices is comparable to AlGaN photoconductors fabricated by MBE or MOVPE.

Acknowledgements This work was partially supported by: the Spanish Government project TEC2015-71127-C2-2-R, the Community of Madrid project S2013/MIT 2790, the Alcalá University project CCG2015/EXP-014 and FPI Grant.

References

[1] J. Wu, W. Walukiewicz, K.M. Yu, J.W. Ager, E.E. Haller, H. Lu, W.J. Schaff, Y. Saito, and Y. Nanishi, Applied Physics Letters 80, 3967 (2002).
[2] W.M. Yim, E.J. Stofko, P.J. Zanzucchi, J.I. Pankove, M. Ettenberg, and S.L. Gilbert, Journal of Applied Physics 44, 292 (1973).
[3] C. Weisbuch, M. Piccardo, L. Martinelli, J. Iveland, J. Peretti, and J.S. Speck, Physica Status Solidi (a) 212, 899 (2015).
[4] A. Yamamoto, M.R. Islam, T.T. Kang, and A. Hashimoto, Physica Status Solidi (C) 7, 1309 (2010).
[5] W.Y. Weng, S.J. Chang, T.J. Hsueh, C.L. Hsu, M.J. Li, and W.C. Lai, Sensors and Actuators B: Chemical 140, 139 (2009).
[6] A. Núñez-Cascajero, Estéban, J.A. Méndez, M. González-Herráez, and F.B. Naranjo, Sensors and Actuators, B: Chemical 223, 768 (2016).
[7] H. Naoi, K. Fujiwara, S. Takado, M. Kurouchi, D. Muto, T. Araki, H. Na, and Y. Nanishi, Journal of Electronic Materials 36, 1313 (2007).
[8] M.J. Lukitsch, Y. V. Danylyuk, V.M. Naik, C. Huang, G.W. Auner, L. Rimai, and R. Naik, Applied Physics Letters 79, 632 (2001).
[9] L. Yun, T. Wei, J. Yan, Z. Liu, J. Wang, and J. Li, Journal of Semiconductors 32, 93001 (2011).
[10] H. Kim-Chauveau, P. de Mierry, J.-M. Chauveau, and J.-Y. Duboz, Journal of Crystal Growth 316, 30 (2011).
[11] A. Núñez-Cascajero, S. Valdueza-Felip, L. Monteagudo-Lerma, E. Monroy, E. Taylor-Shaw, R.W. Martin, M. González-Herráez, and F.B. Naranjo, To be published in Journal of Physics D: Applied Physics.
[12] N. Afzal, M. Devarajan, and K. Ibrahim, Materials Science in Semiconductor Processing 51, 8 (2016).
[13] Q.X. Guo, Y. Okazaki, Y. Kume, T. Tanaka, M. Nishio, and H. Ogawa, Journal of Crystal Growth 300, 151 (2007).
[14] E.T. Yu and M.O. Manasreh, III-V Nitride Semiconductors: Applications and Device (Taylor & Francis, New York, London, 2003).
[15] K.S. Stevens, M. Kinniburgh, and R. Beresford, Applied Physics Letters 66, 3518 (1995).
[16] D. Walker, X. Zhang, P. Kung, A. Saxler, S. Javadpour, J. Xu, and M. Razeghi, Applied Physics Letters 68, 2100 (1996).
[17] E. Muñoz, E. Monroy, J. a. Garrido, I. Izpura, F.J. Sa, and E. Calleja, Applied Physics Letters 71, 870 (1997).
[18] B.K. Li, W.K. Ge, J.N. Wang, and K.J. Chen, Applied Physics Letters 92, (2008).
[19] J.L. Pau, E. Monroy, M.A. Sánchez-García, E. Calleja, and E. Muñoz, Materials Science 93, 159 (2002).
[20] D.K. Wickenden, Z. Huang, D.B. Mott, and P.K. Shu, Johns Hopkins APL Technical Digest (Applied Physics Laboratory) 18, 217 (1997).
[21] L. Monteagudo-Lerma, S. Valdueza-Felip, A. Núñez-Cascajero, A. Ruiz, M. González-Herráez, E. Monroy, and F.B. Naranjo, Journal of Crystal Growth 434, 13 (2016).
[22] H. He, Y. Cao, R. Fu, W. Guo, Z. Huang, M. Wang, C. Huang, J. Huang, and H. Wang, Applied Surface Science 256, 1812 (2010).
[23] J.C. Bernede, J. Pouzet, E. Gourmelon, and H. Hadouda, Synthetic Metals 99, 45 (1999).
[24] E. Monroy, F. Omnes, and F. Calle, Semiconductor Science and Technology 18, R33 (2003).

Copyright line will be provided by the publisher